

The 3CR radio galaxies at $z \sim 1$: Old stellar populations in central cluster galaxies

Philip Best^{1,2}, Malcolm Longair², and Huub Röttgering¹

¹ Sterrewacht Leiden, Huygens Lab, Postbus 9513, 2300 RA, Leiden, The Netherlands

² Cavendish Laboratory, Madingley Road, Cambridge CB3 0HE, England

Abstract. We investigate the old stellar populations of the 3CR radio galaxies at redshift $z \sim 1$ using observations made with the Hubble Space Telescope and the United Kingdom InfraRed Telescope. At radii $r \lesssim 35$ kpc, the infrared radial intensity profiles of the galaxies follow de Vaucouleurs' law, whilst at larger radii the galaxies show an excess of emission similar to that of low redshift cD galaxies. The locus of the high redshift 3CR galaxies on the Kormendy relation is investigated: passive evolution of the stellar populations is required to account for their offset from the relation defined by low redshift giant ellipticals and brightest cluster galaxies. The 3CR galaxies, on average, possess larger characteristic radii than the low redshift brightest cluster galaxies. Coupled with existing evidence, these results are strongly suggestive that distant 3CR galaxies must be highly evolved systems, even at a redshift of one, and lie at the centre of moderate to rich (proto-)clusters.

1 Introduction

The revised 3CR sample of radio sources defined by Laing et al. (1983) consists of the brightest radio sources in the northern sky, selected at 178 MHz. It contains radio galaxies and quasars out to redshifts $z \sim 2$. The low redshift radio galaxies in the sample have long been known to be associated with giant elliptical galaxies containing old stellar populations; if the high redshift sources are similarly associated with giant ellipticals then these sources provide an ideal opportunity to study the evolution of stellar populations at early cosmic epoch, and thus to constrain models of galaxy formation and evolution.

Following the advent of infrared bolometers, Lilly and Longair (1982,1984) obtained infrared K-magnitudes for an almost complete sample of 83 3CR galaxies with redshifts $0 < z < 1.6$. Plotting K magnitude against redshift for these objects, they showed that the resulting relation has a remarkably small scatter ($\lesssim 0.6$ magnitudes). The tightness of this correlation was interpreted as indicating that the high redshift 3CR host galaxies are also giant elliptical galaxies. Lilly and Longair (1984) showed that, unless the deceleration parameter is as large as $q_0 \sim 3.5$, the shape of the K- z relationship is not consistent with non-evolving stellar populations, but that at least passive evolution is required.

The optical-ultraviolet morphologies of the distant galaxies are, however, far more complicated. In 1987, McCarthy et al. and Chambers et al. discovered that the optical emission of powerful high redshift radio galaxies tends to be

elongated and aligned along the direction of the radio emission. Our HST images have allowed us to study the morphologies of these galaxies on kpc scales, and demonstrate that the form of the alignment differs greatly from source to source (Longair et al. 1995, Best et al. 1996, 1997b); in some cases it arises from the elongation of a single central emission region, whilst in others strings of bright knots are seen to stretch along the radio axis. The most promising models for this aligned emission are star formation induced by the radio jet, scattering of quasar light by dust or electrons, or nebular emission from the warm ionised gas (eg. Röttgering and Miley 1996).

2 Spectral energy distributions

The critical point about all of the mechanisms for producing the aligned emission is that they possess relatively flat spectra, and so at the longer wavelengths of the infrared emission they are dominated by the emission of the underlying old stellar population.

To estimate the fraction of the K-band flux density that would arise from the aligned emission, we produce a relatively simple model for the spectral energy distributions (SED's) of the galaxies, using a combination of two components: (i) a passively evolving old stellar population, and (ii) a flat spectrum ($f_\nu \propto \nu^0$) emission component, representing the aligned emission. The SED of the first component was derived using the stellar synthesis codes of Bruzual and Charlot (1993, 1997), assuming that the stars formed in a 1 Gyr burst beginning at a redshift $z = 10$. A Salpeter IMF with upper and lower mass cut-offs of 0.1 and $65M_\odot$ was adopted. The precise spectral shape of the second component of the fit depends upon the nature of the alignment effect; the adoption of a flat spectral index provides a good compromise and will not be too far wrong in any case.

For each galaxy, we calculate the sum of these two components which best matches the broad band flux densities of the galaxies measured at four different wavelengths from our UKIRT and HST images, taking account of any emission line contributions (Best et al. 1997a). 3C437 and 3C470, for which only two broad band flux densities were available, and 3C22 and 3C41 which both possess strong nuclear components in the infrared images (see Section 3) were omitted from this analysis. The fits obtained are generally good. To illustrate this, in Figure 1 we show the results for the first half of the sample. These indicate that the simple two component model provides a good representation of the SED's of these galaxies. The percentage of K-band light associated with the flat spectrum component ranges from only $\sim 1\%$ in the very passive sources 3C65 and 3C337, up to $\sim 22\%$ in the case of 3C368, with an mean value of $\sim 8\%$. Although these percentages would be higher if a redder spectral shape had been adopted for the aligned component, the assumption that the K-band light is dominated by the old stellar population seems reasonably secure.

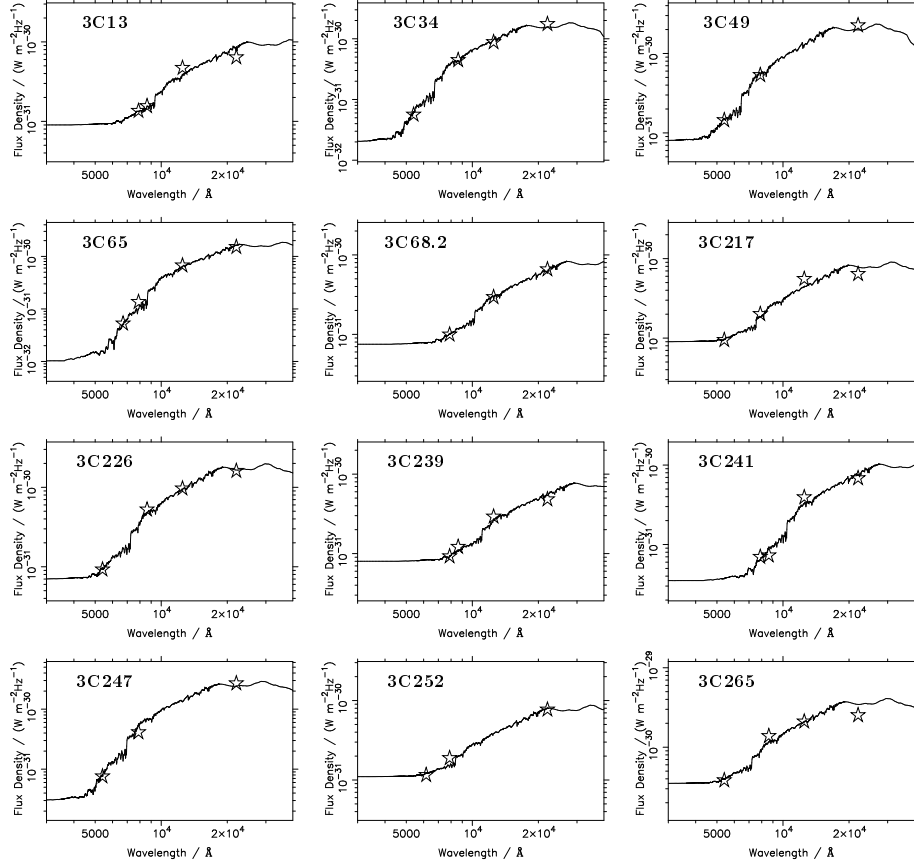


Fig. 1. SED fits to the broad band flux densities of the 3CR galaxies using an old stellar population and a flat spectrum component (see text for details).

3 Radial intensity profiles

Our observations can be used to compare the radial intensity profiles of these galaxies with de Vaucouleurs' law: $I(r) \propto \exp[-7.67(r/r_e)^{-1/4}]$. For 8 of the galaxies in the sample there is little evidence for a significant ultraviolet emission component, in the sense that only a small ($\leq 5\mu\text{Jy}$) flat spectrum component is required in the fit to their SED, and the morphologies of the HST images are almost symmetrical. For these galaxies, the radial profiles of the optical emission were measured, with nearby companion objects being removed and replaced by the average of the background pixels at that distance from the centre of the galaxy. The radial profiles are shown in Figure 2: in 6 of the 8 cases a de Vaucouleurs profile provides an excellent match to the observed data. The cases

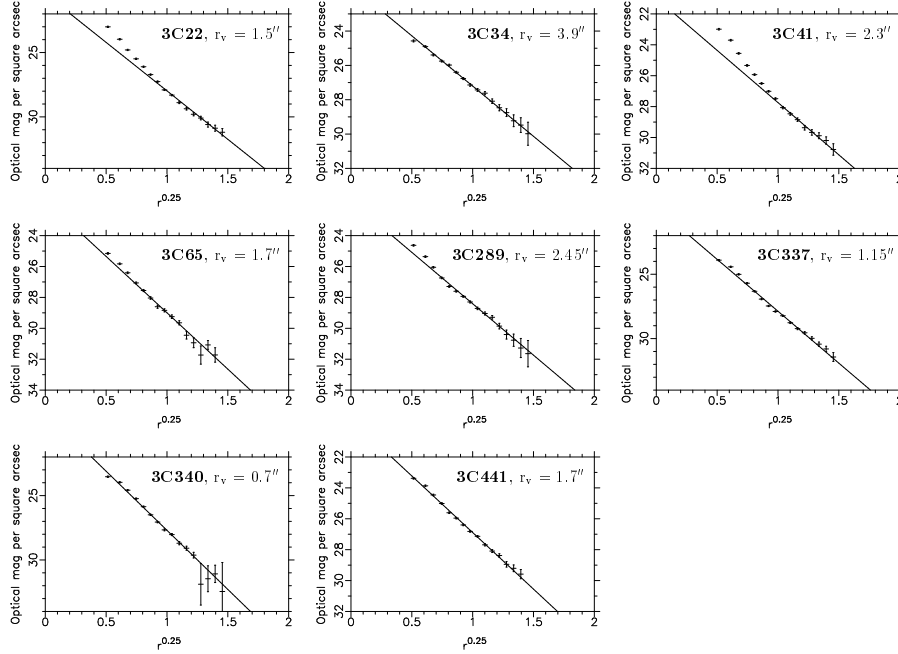


Fig. 2. De Vaucouleurs fits to the radial intensity profiles of the HST images of eight 3CR radio galaxies which do not show a significant active ultraviolet component. The characteristic radius of each, determined from the gradient of the best fitting straight line, is given.

of 3C22 and 3C41 are discussed below. The values of the characteristic radius can typically be measured to an accuracy of order 15%.

Using the characteristic radii determined from the HST images, the infrared profiles of these galaxies can also be investigated. For each of the galaxies, a de Vaucouleurs profile with the characteristic radius derived from the HST fit, and an unresolved emission source were each convolved with effects of the seeing (which was typically between 1 and 1.2 arcsec). The combination of these two components which provided the best match to the observed data was then determined in each case, the results being shown in Figure 3: the dashed line shows the radial profile of the de Vaucouleurs component, the dotted line shows that of the point source component, and the solid line shows the total intensity profile (note that in many cases, the best fit was produced using no point source component, and so this does not appear on the plot). In each case a good match is obtained.

Such fits could also be made for the remaining galaxies in the sample, for which no de Vaucouleurs fit to the HST data was possible due to the aligned emission. For these galaxies, the characteristic radius was allowed to be a further

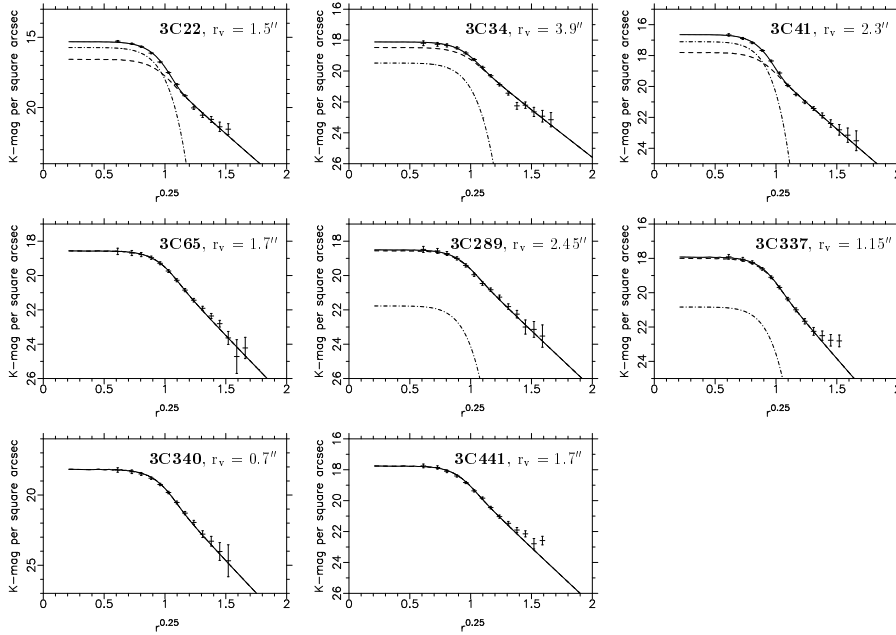


Fig. 3. Fits to the radial intensity profiles of the K–band images of the eight 3CR galaxies shown in Figure 2, using the sum of an unresolved point source (dash–dot line) and a de Vaucouleurs profile with the characteristic radius determined from the HST images (dashed line). For each of the profiles, the effect of seeing has been taken into account. The sum of the two components is indicated by the solid line. (Note that in many cases the best fit does not involve a point source component.)

free parameter in the fit. For the five galaxies with redshifts $z > 1.4$, the low signal–to–noise ratio of the infrared images meant that the χ^2 of the fit varied only slowly with characteristic radius and so the best–fitting characteristic radius was not well–defined; these galaxies have therefore been omitted from the analysis. For the remaining galaxies the characteristic radius could typically be determined to an accuracy of $\sim 35\%$, and the best fitting models are shown in Figure 4.

Figures 3 and 4 demonstrate that, except for the two cases of 3C22 and 3C41, there is only a small ($< 10\%$) point source component contributing to the total K–band flux density of the 3CR radio galaxies. Indeed, the point source contribution is consistent, within the 90% confidence limits, with being zero in all but these two cases. For 3C22 and 3C41, approximately 37% and 24% (respectively) of the K–band emission is associated with an unresolved emission source. It is interesting to note that these two galaxies are the brightest in our sample in the K–band, lying furthest from the mean K– z relationship (Best et al. 1997a).

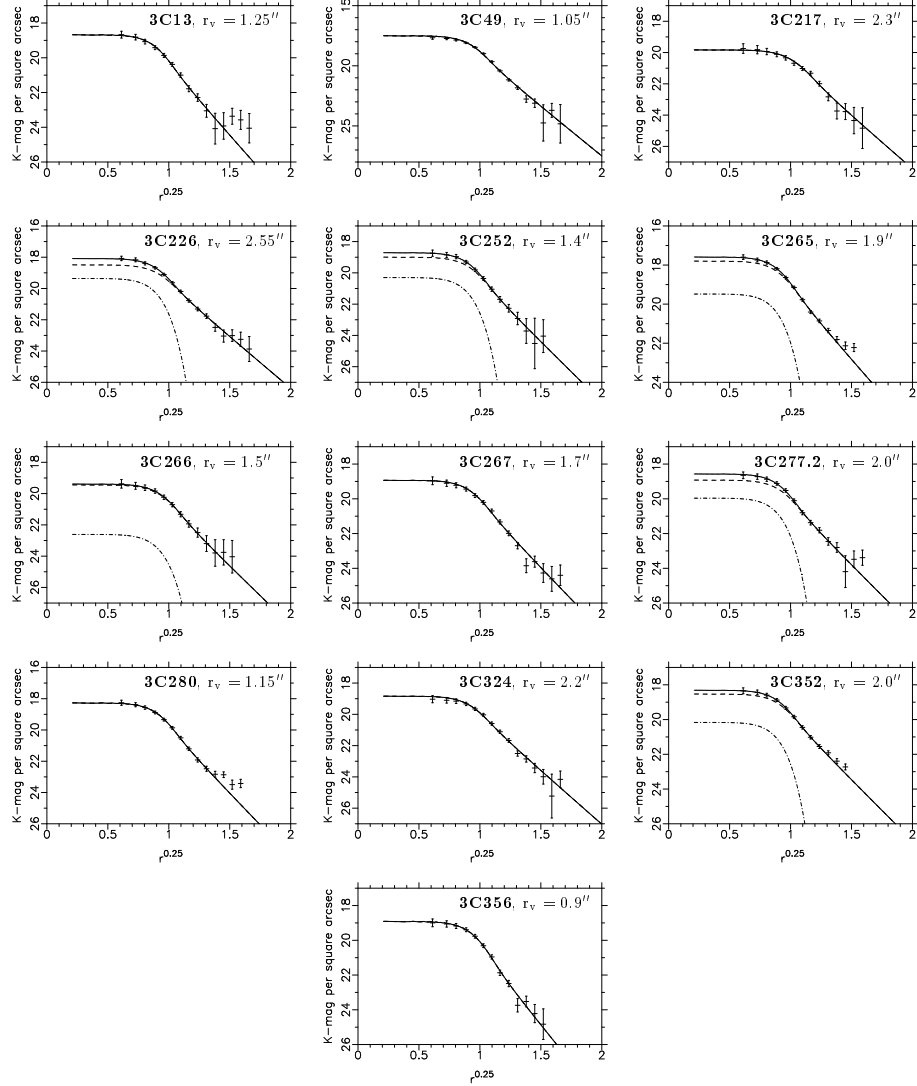


Fig. 4. Fits to the radial intensity profiles of the K-band images of the 13 3CR galaxies for which enhanced optical emission prevented such a fit to the optical intensity profile. The characteristic radii have been determined from the best fitting profiles. The same notation is used as in Figure 3.

Rawlings et al. (1995) have previously proposed that 3C22 possesses a significant unresolved K-band contribution and, together the detection of broad $H\alpha$ emission (Economou et al. 1995) from this galaxy, this suggests that this source may be a reddened quasar.

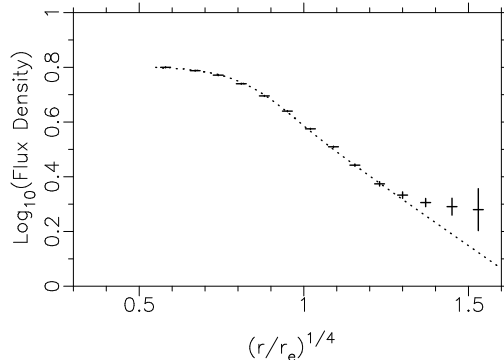


Fig. 5. A combined radial intensity profile in the K-band for the 12 galaxies with $1.0 \leq r_e \leq 2.0$. Units on the y-axis are arbitrary. Errors for each point are marked. The dotted line shows a combined de Vaucouleurs profile: halo emission is clearly visible at $(r/r_e)^{1/4} \gtrsim 1.25$.

It is noticeable that for a proportion of the galaxies the observed emission profile becomes brighter than the predicted de Vaucouleurs profile at large radii, suggesting that these galaxies possess diffuse extended envelopes. To improve the signal-to-noise of this feature, we have scaled the radial profile of each galaxy with respect to the characteristic radius derived for it, and summed the intensity profiles. Only those galaxies for which $1.0 \leq r_e \leq 2.0$ were included: for galaxies with a smaller r_e there will still be a significant effect due to the seeing at radii of 2 to 3 r_e , whilst for galaxies with a larger r_e there is insufficient signal at the largest radii to accurately test for the presence of the halo. For the 12 galaxies which meet this criteria, the scaled radial profiles were summed, weighting each galaxy equally, and the results are presented in Figure 5. At radii $(r/r_e)^{1/4} \gtrsim 1.25$, corresponding to $r \gtrsim 35$ kpc, there is a clearly significant halo component.

This halo component is very similar to that of low redshift cD galaxies, which lie towards the centre of galaxy clusters. Together with the large (a few times $10^{11} M_\odot$) masses of these galaxies, this suggests that high redshift 3CR galaxies may live in moderately rich environments. Existing evidence supports this hypothesis, eg. the detection of cooling flows around these galaxies (Crawford and Fabian 1995), evidence for companion galaxies in narrow-band [OII] images (McCarthy 1988), and the fact that individual well-studied 3CR galaxies at high redshift appear to live in clusters (eg. 3C324, Dickinson et al. 1996).

4 The Kormendy relation for the redshift one 3CR radio galaxies

The Kormendy r_e vs μ_e projection of the fundamental plane alleviates the need for detailed spectroscopy, which is a difficult process for high redshift galaxies. In the previous section we obtained good estimates for the characteristic radii of the 3CR galaxies; by measuring also their surface brightnesses, it will be possible to compare their location on the Kormendy projection with those of low redshift brightest cluster galaxies and giant ellipticals. Thus, we can investigate how much evolution of the stellar populations must be occurring with cosmic epoch.

There are a number of details which need to be dealt with before the location of the 3CR galaxies on the Kormendy relation can be determined. The foremost of these is that we can not use the HST images to measure the surface brightnesses, because of the large component of light associated with the aligned emission at these wavelengths. Instead, the K-band images must be used, with the adoption of an appropriate k-correction. We must also take account of the effects of seeing in the K-band observations, of any point source or flat spectrum contributions to the flux density (as calculated in the earlier sections of this paper), and compensate for cosmological surface brightness dimming.

As a first, null hypothesis, we assume that the stellar populations of the 3CR radio galaxies are not evolving, and so we use the SED of low redshift giant elliptical galaxies to calculate the required k-correction. The rest-frame B-band surface brightnesses thus calculated for the 3CR radio galaxies are plotted against the measured de Vaucouleurs radii in Figure 6a, together with data from low redshift samples of giant ellipticals and brightest cluster galaxies (Oegerle and Hoessel 1991, Schombert 1987) and a sample of low redshift radio galaxies (Lilly and Prestage 1987). The 3CR galaxies have greater surface brightnesses than the low redshift galaxies in the fundamental plane, implying that some stellar evolution must have occurred between a redshift of one and the current epoch.

We can repeat the process, but instead make the more physical assumption that the stellar populations of the 3CR radio galaxies form at high redshift ($z = 10$) and then evolve passively. If evolution is occurring, the stellar populations observed in the high redshift radio galaxies will be younger, and hence brighter, than those seen in the nearby galaxies. The Bruzual and Charlot (1993, 1997) stellar synthesis codes were used to construct such passively evolving galaxies with the age that each 3CR galaxy would possess, and thus to calculate the required k-correction. The models were then used to determine the evolution in the rest-frame B-magnitude of the stellar populations that would occur for each galaxy between its observed redshift and a redshift of zero. This procedure therefore derived surface brightnesses of the 3CR galaxies that could be compared directly with low redshift giant ellipticals in the fundamental plane.

The derived surface brightnesses are plotted against the de Vaucouleurs radius in Figure 6b. It can be seen that they lie along the fundamental plane defined by the low redshift giant ellipticals, providing further evidence that the

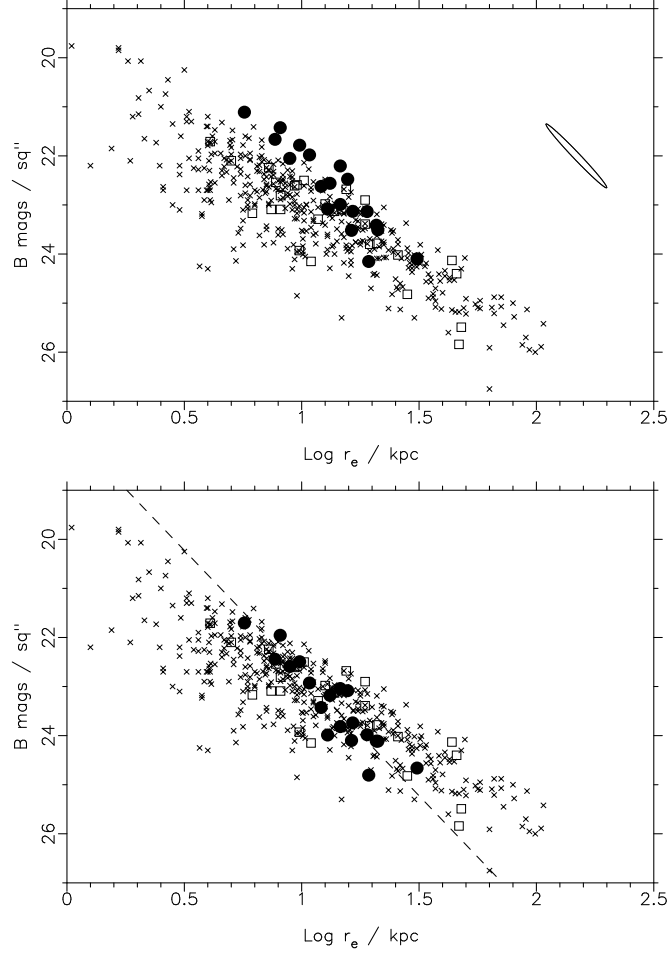


Fig. 6. Plots of B-band surface brightness vs characteristic radius for the 3CR galaxies (solid circles) compared with low redshift giant ellipticals and brightest cluster galaxies (crosses), and low redshift radio galaxies (open squares). The low redshift data are taken from Rigler and Lilly (1994) and references therein. The ellipse indicates the error ellipse for the 3CR galaxies whose characteristic radius was measured from the UKIRT data; those for which the measurement was from the HST data have much an error ellipse less than half of this size. (a) Assuming no evolution of the stellar populations of the 3CR galaxies. (b) Assuming that the stellar populations evolve passively. The dashed line shows a line of constant total luminosity.

stellar populations evolve passively. There is an indication that the slope of the fundamental plane defined by the 3CR galaxies may be slightly steeper than that of the low redshift giant ellipticals, but this is likely to be just a selection

effect: the dashed line on Figure 6b shows a line of constant total luminosity for the galaxies, that is, a line along which the product of the surface brightness and the square of the characteristic radius is constant; the 3CR galaxies lie closely along this line. That is, they lie within the fundamental plane, and also along the line of constant luminosity.

According to standard cannibalism models (eg. Hausman and Ostriker 1978) the position of a galaxy along the fundamental plane is interpreted as being related to its merger history. Galaxies which have undergone more mergers and are more highly evolved lie further to the right along the fundamental plane. In this respect it is interesting to note that: (i) on Figure 6, the high redshift 3CR galaxies possess a smaller spread of characteristic radii than those of the low redshift samples, indicating perhaps that these galaxies are all seen at a similar point in their evolutionary history, and (ii) the mean characteristic radius of the 3CR galaxies (14.6 ± 1.4 kpc) is larger than that of the low redshift samples (11.0 ± 0.5 kpc). This indicates that the 3CR galaxies must be highly evolved systems, even by a redshift of one.

5 Conclusions

From our study of the high redshift 3CR radio galaxies, we conclude the following points:

- The radial intensity profiles of the host galaxies of the 3CR radio sources are well matched by de Vaucouleurs' law.
- The galaxies possess extended cD type halos.
- Passive evolution of the stellar populations is required if the 3CR galaxies are to lie along the fundamental plane defined by low redshift giant ellipticals.
- Their characteristic radii are large, with relatively little scatter.

We conclude that the 3CR radio galaxies at redshift $z \sim 1$ are highly evolved galaxies, containing old stellar populations, which lie at the centre of moderately rich (proto-)clusters.

References

- Best P. N., Longair M. S., Röttgering H. J. A., 1996, MNRAS, **280**, L9
 Best P. N., Longair M. S., Röttgering H. J. A., 1997a, MNRAS: *in press*.
 Best P. N., Longair M. S., Röttgering H. J. A., 1997b, MNRAS: *submitted*.
 Bruzual G., Charlot S., 1993, ApJ, **405**, 538
 Bruzual G., Charlot S., 1997, *submitted*
 Chambers K. C., Miley G. K., van Breugel W. J. M., 1987, Nature, **329**, 604
 Crawford C. S., Fabian A. C., 1995, MNRAS, **273**, 827
 Dickinson M., Dey A., Spinrad H., 1996, *Galaxies in the Young Universe*, Hippelein H. ed, Spinger Verlag, *in press*
 Economou F., Lawrence A., Ward M. J., Blanco P. R., 1995, MNRAS, **272**, L5
 Hausman M. A., Ostriker J. P., 1978, ApJ, **224**, 320

- Laing R. A., Riley J. M., Longair M. S., 1983, MNRAS, **204**, 151
Lilly S. J., Longair M. S., 1982, MNRAS, **199**, 1053
Lilly S. J., Longair M. S., 1984, MNRAS, **211**, 833
Lilly S. J., Prestage R. M., 1987, MNRAS, **225**, 531
Longair M. S., Best P. N., Röttgering H. J. A., 1995, MNRAS, **275**, L47
McCarthy P. J., van Breugel W. J. M., Spinrad H., Djorgovski S., 1987, ApJ, **321**, L29
McCarthy P. J., 1988, PhD Thesis, University of California, Berkeley
Oegerle W. R., Hoessel J. G., 1991, ApJ, **375**, 15
Rawlings S., Lacy M., Sivia D. S., Eales S. A., 1995, MNRAS, **274**, 428
Rigler M. A., Lilly S. J., 1994, ApJ, **427**, L79
Röttgering H. J. A., Miley G. K., 1996, *The Early Universe with the VLT*, Bergeron J. ed, Springer Verlag, *in press*
Schombert J. M., 1987, ApJ Supp., **64**, 643